J. Fluid Mech. (2006), *vol.* 554, *pp.* 433–456.
doi:10.1017/S0022112006009001 Printed in the United Kingdom

Statistical mechanics of two-dimensional turbulence

By SUNGHWAN JUNG[1], P. J. MORRISON[2] AND HARRY L. SWINNEY[1]

[1]Center for Nonlinear Dynamics and Department of Physics, The University of Texas at Austin, Austin, TX 78712, USA

[2]Institute for Fusion Studies and Department of Physics, The University of Texas at Austin, Austin, TX 78712, USA

(Received 11 March 2005 and in revised form 20 December 2005)

The statistical mechanical description of two-dimensional inviscid fluid turbulence is reconsidered. Using this description, we make predictions about turbulent flow in a rapidly rotating laboratory annulus. Measurements on the continuously forced, weakly dissipative flow reveal coherent vortices in a mean zonal flow. Statistical mechanics has two crucial requirements for equilibrium: statistical independence of macro-cells (subsystems) and additivity of invariants of macro-cells. We investigate these requirements in the context of the annulus experiment. The energy invariant, an extensive quantity, should thus be additive, i.e. the interaction energy between a macro-cell and the rest of the system (reservoir) should be small, and this is verified experimentally. Similarly, we use additivity to select the appropriate Casimir invariants from the infinite set available in vortex dynamics, and we do this in such a way that the exchange of micro-cells within a macro-cell does not alter an invariant of a macro-cell. A novel feature of the present study is our choice of macro-cells, which are continuous phase-space curves based on mean values of the streamfunction. Quantities such as energy and enstrophy can be defined on each curve, and these lead to a local canonical distribution that is also defined on each curve. The distribution obtained describes the anisotropic and inhomogeneous properties of a flow. Our approach leads to the prediction that on a mean streamfunction curve there should be a linear relation between the ensemble-averaged potential vorticity and the time-averaged streamfunction, and our laboratory data are in good accord with this prediction. Further, the approach predicts that although the probability distribution function for potential vorticity in the entire system is non-Gaussian, the distribution function of micro-cells should be Gaussian on the macro-cells, i.e. for curves defined by mean values of the streamfunction. This prediction is also supported by the data. While the statistical mechanics approach used was motivated by and applied to experiments on turbulence in a rotating annulus, the approach is quite general and is applicable to a large class of Hamiltonian systems, including drift-wave plasma models, Vlasov–Poisson dynamics, and kinetic theories of stellar dynamics.

1. Introduction

1.1. *Overview*

Statistical mechanics provides a way to calculate the macroscopic properties of matter from the behaviour of microscopic constituents. Instead of considering all motions of the individual constituents, one describes observable quantities averaged over constituent Hamiltonian trajectories, and averages are evaluated using the probability

distribution of possible microstates. Likewise, fluid systems with a local balance between dissipation and forcing have been described by statistical mechanics with the inclusion of constraints based on invariants of the dynamics. In general, such statistical theories for fluids are based on the idea that the macroscopic behaviour of the fluid turbulence can be described without knowing detailed information about small-scale vortices.

The justification of statistical mechanics based on ideal two-dimensional fluid equations is open to question, given the existence of forcing, dissipation, three-dimensional effects, temperature gradients, etc., that certainly occur in real fluid flows. Moreover, one must square the idea of cascading with the approach to statistical equilibrium. Ultimately, such a justification is very difficult and would rely on delicate mathematical limits. However, its success amounts to the idea that the fluid system can in some sense be described by weakly interacting subsystems, where the behaviour of a single subsystem can be described by weak coupling to a heat bath that embodies all of the other subsystems and all of the omitted effects. In the end 'the proof of the pudding is in the eating', and our justification is based on experimental observations.

Intimately related to the existence of subsystems is the question of which invariants to incorporate into a statistical mechanics treatment of fluids. One aim of the present paper is to investigate this question. We do this both conceptually and experimentally and come to the conclusion that quadratic invariants (energy and enstrophy) are most important. Our conclusion follows from the observation that these invariants possess the property of additivity.

The microscopic dynamics of conventional statistical mechanics is finite-dimensional, but to describe macrosopic phenomena one takes the thermodynamic limit in which the number of degrees of freedom tends to infinity. However, the dynamics of a two-dimensional fluid is already infinite-dimensional and possesses an infinite number of invariants; so, in order to make progress with a statistical mechanics approach one must extract a finite-dimensional model, and such a model cannot conserve all of the invariants of the original fluid system. In calculations one may also take limits of this finite-dimensional model, but the results of these limits may depend upon which of the invariants are maintained. Additivity of macroscopic invariants and statistical independence of subsystems are crucial properties in conventional statistical mechanics (see e.g. Landau & Lifshitz 1980). Because not all invariants of a system are additive, this property can be used to select invariants for statistical mechanics from the infinite number possessed by two-dimensional fluid systems.

Related to the choice of additive invariants is the choice of subsystems. This choice requires the identification of two scales, a macroscopic scale and a microscopic scale, which we call Δ and δ, respectively, and phase-space cells of these characteristic sizes are considered. In classical statistical mechanics, the micro-cells usually refer to individual particles, while the macro-cells, the subsystems, are selected to be large enough to contain many particles yet small enough to have uniform invariants. We address in detail the choice of these cells for the fluid in § 5, but it is clear that a macro-cell should contain many micro-cells, yet be small enough so that the vorticity and streamfunction are constant. This condition is sufficient for statistical independence, but the converse is not always true. In any event we seek to define macro-cells that are nearly statistically independent and consider only invariants that are additive over these cells.

A second aim of the present work is to propose the idea that temporal mean values of the streamfunction provide a natural coordinate system for describing inhomogeneous turbulence, a coordinate system that can be used to define statistically independent subsystems. We suggest this idea because contours of the streamfunction

for two-dimensional inviscid fluid flow tend to be smooth and because there tends to be a strong statistical dependence of vorticity or potential vorticity along those contours. Streamfunction contours are much smoother than vorticity contours because of the smoothing property of the inverse Laplacian. Therefore, there is a natural separation of length scales: the large scale associated with variation of the streamfunction contours and the fine scale that is needed to resolve the vorticity or potential vorticity. We take these to be our scales Δ and δ, respectively. We test this idea experimentally by measuring the independence of subsystems so defined. We then construct a theory based on this definition of subsystem together with the additivity of quadratic invariants, and compare its predictions with the measured vorticity probability density function.

1.2. *Background*

In a remarkable series of papers Burgers (1929*a–c*, 1933*a–d*) (reprinted in Nieuwstadt & Steketee 1995) appears to be the first researcher to apply statistical mechanics ideas to the description of fluid turbulence. Many basic ideas used by later researchers were introduced first by Burgers in these rarely cited papers. Burgers introduced both lattice and Fourier models and showed that such models satisfy Liouville's theorem when viscosity is neglected. He used a counting argument to derive an entropy expression and obtained a corresponding entropy maximization principle. He proposed a microscopic scale for describing turbulent motion during short intervals of time and defined macroscopic quantities by counting possible streamfunction realizations for sequences of time intervals. His analysis is based on the Reynolds stress equation, and he obtained a probability distribution that can be used to calculate the mean value of the Reynolds stress.

Motivated by the work of Burgers, Onsager (1949) took up the subject and considered a representation of the vorticity field in terms of a set of point vortices, zero-area vortices, of equal strength. Because this results in a finite-dimensional particle-like Hamiltonian system, Onsager could proceed to apply techniques of classical statistical mechanics. He gave arguments for the existence of negative temperatures and the occurrence of coherent structures in a confined region, which are often observed in nature. Related ideas have been further pursued by many researchers, e.g. Joyce & Montgomery (1973), Matthaeus *et al.* (1991), Eyink & Spohn (1993), Yin, Clercx & Montgomery (2004) (see Eyink & Sreenivasan (2006) for a recent review). For example, Joyce & Montgomery (1973) studied the statistical mechanics of point vortices within a mean field approximation, and argued that in the negative temperature regime, large like-signed vortices are the most probable state.

Lee (1952) projected three-dimensional fluid equations (including magnetohydrodynamics) onto a Fourier basis and truncated to obtain a finite-dimensional system. Evidently unaware of the early work of Burgers (1933*d*), he again demonstrated that his truncated system satisfies a version of Liouville's theorem and was thus amenable to techniques of statistical mechanics. Later, Kraichnan considered two-dimensional fluids (Kraichnan 1967, 1975; Kraichnan & Montgomery 1980) and noted that out of the infinite number of invariants, two quadratic ones, the so-called rugged invariants, remained invariants after truncation. Kraichnan & Montgomery argued that these rugged invariants are the important ones, and obtained an equilibrium state, which is related to that obtained by minimum-enstrophy arguments put forth by selective decay hypotheses (Leith 1984; Maxworthy 1984; Bouchet & Sommeria 2002). Also, using Kolmogorov-like dimensional arguments and the rugged invariants, Kraichnan argued for the existence of direct and inverse cascades for two-dimensional turbulence (Kraichnan 1967).

The two-dimensional Euler equation, like the Vlasov and other transport equations, can be viewed as mean field theory. Such equations are known to generate fine structure in the course of evolution. This led Lynden-Bell (1967) to consider a coarse-graining procedure coupled with the idea of preserving all of the infinity of invariants such theories possess. He applied his ideas in the context of stellar dynamics, but the ideas are akin to those used in treatments of the classical electron gas by generalizations of Debye–Hückle theory (e.g. Van Kampen & Felderhof 1967). Later, such ideas were used in the fluid context by Robert (1991), Robert & Sommeria (1991, 1992), Miller (1990), and Miller, Weichman & Cross (1992), and again in the stellar dynamics context by Chavanis, Sommeria & Robert (1996). Our development to a significant extent parallels that of these authors. In these works a microscopic probability distribution represents a local description of the small-scale fluctuations of microscopic vortices. The streamfunction is assumed to be uniform on the microscopic scale, and an equilibrium state is obtained by maximizing the Boltzmann entropy of microstates, an entropy that is obtained by a counting argument first given by Lynden-Bell. This produces a most probable state.

More recently, the necessity of incorporating the infinite number of invariants in statistical mechanics theories has been brought into question, and theories based on finite-dimensional models with fewer constraints have been developed. Majda & Holen (1997) have argued that including an infinite number of invariants provides no additional statistical information, and Turkington (1999) has argued that previous theories have not properly handled the neglected small-scale phenomena, and he has proposed a theory that uses inequality constraints associated with only the convex invariants. Our approach is perhaps most closely aligned to these works, but is distinguished by the fact that the invariants chosen are explicitly based on the additivity argument, the choice of subsystems, and experimental observation.

Natural phenomena in atmospheres and oceans have served as a motivation for the application of statistical mechanics to two-dimensional fluid flow (e.g. Salmon, Holloway & Henderschott 1976). Examples include zonal flows in planets, such as the jet stream and the polar night jet, and organized coherent vortices, such as the Great Red Spot of Jupiter (Maxworthy 1984; Sommeria, Meyers & Swinney 1988, 1991; Marcus 1993; Bouchet & Sommeria 2002). Attempts have been made to explain such naturally occurring phenomena in terms of the coherent structures found to emerge in quasi-geostrophic and two-dimensional turbulence after long-time evolution. With external small-scale forcing a few long-lived and large structures resulting from nonlinear merging processes are seen to be stable self-organized states that persist in a strongly turbulent environment (McWilliams 1984; Boucher, Ellis & Turkington 2000). These structures have been studied over many years, often because of their relevance to large-scale geophysical and astrophysical flows (Marcus 1993). In statistical mechanics, such steady states with large structures are envisioned to be the most probable state arising from some extremization principle. Various extremization principles (e.g. Leith 1984) have been proposed with selected global invariants of the system used as constraints. Observations of turbulent flow with large coherent structures in a rotating annulus (Sommeria *et al.* 1988; Baroud *et al.* 2002, 2003; Aubert, Jung & Swinney 2002; Jung *et al.* 2004) have led us to reconsider statistical mechanics in the context of rapidly rotating systems.

1.3. *Notation and organization*

By necessity this paper contains much notation. To aid the reader we give a brief summary here. As noted above, statistical mechanics deals with two scales: the

microscopic scale δ, characteristic of microscopic m-cells, and the macroscopic scale Δ, characteristic of macroscopic M-cells. Several averages are considered. The symbol $\langle \cdot \rangle_S$ denotes an average with probability density P_S, where choices for the subscript S will be used to delineate between different cases. The appropriate volume measure will be clear from the context but is also revealed by the argument of P_S. Averages with uniform density are denoted by $\prec \cdot \succ_S$, where the subscript denotes the integration variable. An exception is the time average, which we denote by an overbar. Thus, the time average of a function is denoted by $\bar{f}$, and $\bar{f} = \int_0^T f \, \mathrm{d}t/T = \prec f \succ_t$. The limits of integration for this kind of average will either be stated or will be clear from the context. We denote the potential vorticity field by $q(x, y, t)$, by which we always mean a function. For the potential vorticity distribution on an M-cell (subsystem) we use ζ, an independent variable. Another source of possible confusion is that the symbol β is used for the energy Lagrange multiplier, as is conventional in statistical mechanics, while the beta-effect of geophysical fluid dynamics is embodied here in the symbol h.

The paper is organized as follows. The experiment is described in § 2 and equations that govern the dominant physics are reviewed in § 3. In § 4 we describe some basic ideas about statistical mechanics, as needed for the application to the fluid system of interest. In § 5 we describe statistical mechanics in the mean field approximation and compare predictions with experiments. Here we show that predictions of the theory are in accordance with experiments. Finally, in § 6 we conclude.

2. Experiment

The experiments are conducted in a rotating annulus (figure 1). The annulus has an inner radius $r_i = 10.8$ cm, outer radius $r_o = 43.2$ cm, a sloping bottom, and a flat transparent lid. The bottom depth varies from 17.1 cm at the inner radius to 20.3 cm at the outer radius, giving a bottom slope of $\eta = -0.1$. For the data analysed in this paper, the rotation frequency of the annulus is $\Omega/2\pi = 1.75$ Hz. An azimuthal jet is generated in the annulus by pumping water in a closed circuit through two concentric rings of holes at the bottom. Fluid is pumped into the annulus through an inner ring at $r = 18.9$ cm and extracted through an outer ring at $r = 35.1$ cm; both rings have 120 circular holes. Each hole has a diameter of 2.5 mm, and the total pumping rate is $150\,\mathrm{cm^3\,s^{-1}}$. The action of the Coriolis force on the outward flux generates a counter-rotating azimuthal jet. A counter-rotating flow is generally more unstable than a co-rotating flow (Sommeria *et al.* 1991).

The water is seeded with neutrally buoyant particles (polystyrene spheres, diameter 150–200 μm). Light-emitting diodes produce a 3 cm thick horizontal sheet of light that illuminates the annulus at mid-depth. The particles suspended in the water are imaged with a camera located 2 m above the annulus, and the camera rotates with the tank. Particle image velocimetry (PIV) is used to obtain the full two-dimensional velocity field (Baroud *et al.* 2003).

The flow can be characterized by the Reynolds, Rossby, and Ekman numbers. The maximum velocity $U_{\max} \approx 22\,\mathrm{cm\,s^{-1}}$, the length $L = 16.2$ cm (taken to be the distance between the two forcing rings) and the kinematic viscosity $\nu = 0.01\,\mathrm{cm^2\,s^{-1}}$ yield a Reynolds number $UL/\nu = 3.5 \times 10^4$, indicating that the flow is turbulent. The Rossby number (ratio of inertial to Coriolis force) is $\omega_{rms}/2\Omega = 0.11$ (where ω_{rms} is the r.m.s. vorticity), which indicates that the Coriolis force is dominant, as is the case for planetary flows on large length scales. Finally, the small Ekman number, $\nu/2L^2\Omega = 3 \times 10^{-4}$, indicates that dissipation in the bulk is small. The Ekman time, $\tau_E = L_h/2(\nu\Omega)^{1/2}$ (where L_h is the mean fluid height) for dissipation in the boundary

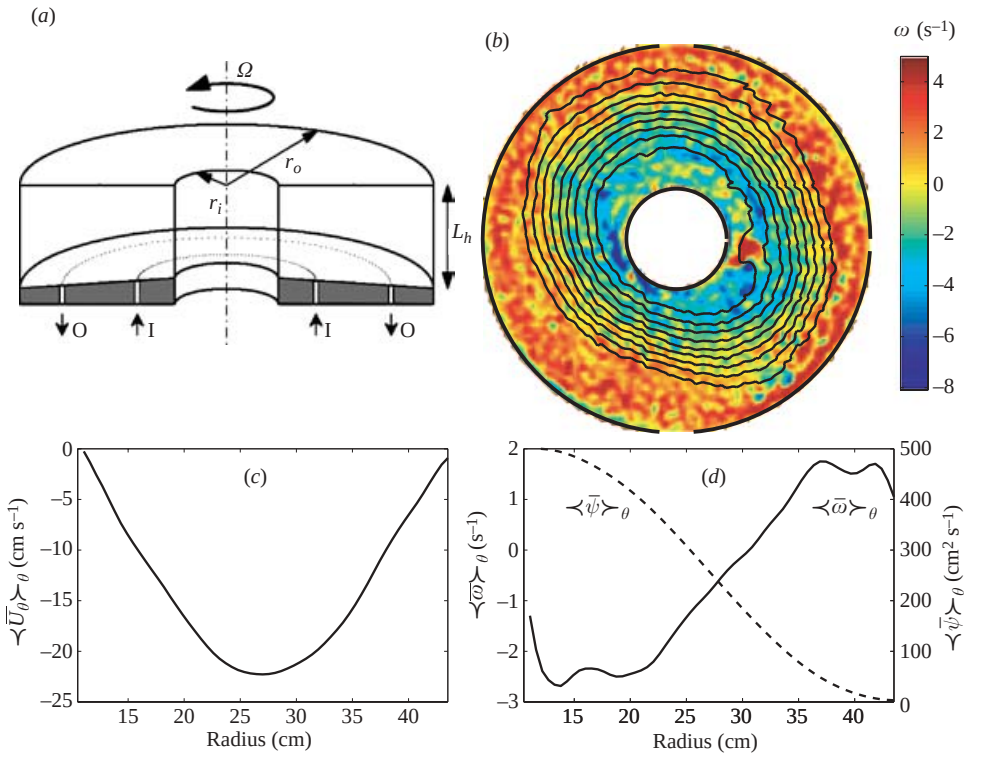

FIGURE 1. (*a*) Schematic diagram of the experimental apparatus. The tank rotates at 1.75 Hz. Flow is produced by pumping water through a ring of inlets (I) and outlets (O) in the bottom of the tank. The Coriolis force acts on the radially pumped fluid to produce a counter-rotating jet. (*b*) The vorticity field and contours of streamfunction at mid-height of the tank, determined from particle image velocimetry measurements. The streamfunction contours are equally spaced in streamfunction value. (*c*) The azimuthal velocity averaged over both time and azimuthal angle, as a function of radial position. (*d*) The vorticity (solid line) and streamfunction (dashed line) averaged over time and azimuthal angle, as a function of radial position.

layers is 30 s, a time much longer than the typical vortex turnover time, 2 s. The dimensionless numbers indicate that the flow is quasi-geostrophic; previous studies of turbulence in the annulus have indeed confirmed the strong two-dimensionality of the flow (Baroud *et al.* 2003)

3. Dynamics

The barotropic assumption is widely used to describe the flow inside the tank. The equation of motion for a barotropic fluid with topography is given by

$$\frac{\partial q}{\partial t} + \boldsymbol{u}\cdot\nabla q = D + F\,, \tag{3.1}$$

where $q = (-\nabla^2\psi + 2\Omega)/L_h$ is the potential vorticity, L_h is the tank depth, ψ is the streamfunction, $\boldsymbol{u} = (\partial\psi/\partial y, -\partial\psi/\partial x)$, D denotes dissipation, such as that due to molecular viscosity, $\nu\nabla^2\omega$, or Ekman drag, $-\omega/\tau_E$, and F denotes a vorticity source due to the pumping. Often the potential vorticity is approximated by

$$q = -\nabla^2\psi + h\,, \tag{3.2}$$

where h accounts for the beta-effect and is here a linear function of radius, $h = 2\Omega\eta r/L_h$ where η is the bottom slope. Over the years strong evidence has accumulted that (3.1) describes the dominant features of the experiment (Sommeria *et al.* 1991; del-Castillo-Negrete & Morrison 1992; Meyers, Sommeria & Swinney 1993; Solomon, Holloway & Swinney 1993).

For inviscid flow with zero Rossby number, there is no vertical variation in the velocity (Rossby 1939), and there is evidence that to leading order the drag and forcing terms cancel. We are primarily interested in the statistics of motions that occur on the vortex turnover time, and these are governed by the inviscid equation,

$$\frac{\partial q}{\partial t} + \boldsymbol{u}\cdot\nabla q = 0, \tag{3.3}$$

which is a Hamiltonian theory.

A manifestation of the Hamiltonian nature of two-dimensional Euler-like flows such as (3.3) is the finite-dimensional Hamiltonian description of point vortices provided by Kirchhoff (1883), which played an essential motivating role in Onsager's theory (e.g. Eyink & Sreenivasan 2006). For a distributed vorticity variable such as q the Hamiltonian form is infinite-dimensional and is given in terms of a non-canonical Poisson bracket as follows:

$$\frac{\partial q}{\partial t} = \{q, H\} = [\psi, q], \tag{3.4}$$

where the Hamiltonian $H[q] = \int \psi(q - h)\,\mathrm{d}x\,\mathrm{d}y/2$, and the non-canonical Poisson bracket is given by

$$\{F, G\} = \int q\left[\frac{\delta F}{\delta q}, \frac{\delta G}{\delta q}\right]\mathrm{d}x\,\mathrm{d}y, \tag{3.5}$$

with F and G being functionals, $\delta F/\delta q$ the functional derivative, and $[f, g] = f_x g_y - f_y g_x$. Observe that $\boldsymbol{u}\cdot\nabla q = -[\psi, q]$. This Hamiltonian formulation of the two-dimensional Euler equation appeared in (Morrison 1981*a*,*b*, 1982), based on the identical structure for the Vlasov–Poisson system (Morrison 1980), and in Olver (1982). A review of this and other forumlations can be found in Morrison (1998). The infinite family of Casimir invariants $C[q] = \int \mathscr{C}(q)\,\mathrm{d}x\,\mathrm{d}y$, where $\mathscr{C}$ is arbitrary, satisfies $\{F, C\} = 0$ for all functionals F, and is thus conserved by (3.3). The presence of these invariants is one way that the statistical mechanics of fluids differs from that of particle systems.

4. Statistical mechanics and fluid mechanics

As noted in § 1, many attempts have been made to apply statistical mechanics to fluids and other infinite-dimensional systems. In this section we describe our notation and discuss some basic ideas.

4.1. *State variables*

In classical statistical mechanics the microscopic dynamics is governed by Hamilton's equations and the phase space is the $2N$-dimensional manifold with canonical coordinates (Q_α, P_α), $\alpha = 1, 2, \ldots, N$, where $(Q_1, \ldots Q_N)$ is the configuration coordinate and $(P_1, \ldots, P_N)$ is the corresponding canonical momentum. Typically N, the number of degrees of freedom, is a very large number $\sim 10^{23}$. We call this $2N$-dimensional phase space Γ, a standard notation introduced by Ehrenfest & Ehrenfest (1959). Our fluid is assumed to be governed by (3.3), an infinite-dimensional

Hamiltonian theory, and thus the instantaneous state of our system is determined by the vorticity-like variable $q(x, y)$, which we suppose is contained in some space of functions $\mathscr{G}$. The index α for coordinates of Γ is analogous to the Eulerian position (x, y), a point in the physical domain occupied by the fluid, which is viewed as an index for $\mathscr{G}$.

In conventional statistical mechanics, the microscopic dynamics is finite-dimensional, and one attempts to explain phenomena on the macroscopic level by considering the thermodynamic limit in which $N \to \infty$. However, for a fluid, the dynamics is already infinite-dimensional, and thus as noted in § 1, to apply statistical mechanics researchers have introduced various finite-dimensional discretizations. Onsager's description of the continuum vortex dynamics in terms of a collection of point vortices amounts to the specification of the coordinates of the manifold analogous to Γ as the spatial positions of the point vortices, $(x_1, \ldots x_N, y_1, \ldots, y_N)$. Alternatively, Lee's representation of a three-dimensional fluid in terms of a truncated Fourier series has the Fourier amplitudes being coordinates of a space analogous to Γ. This procedure was carried over to two dimensions by Kraichnan & Montgomery (1980). For our potential vorticity variable the Fourier amplitudes are given by $q_{\boldsymbol{k}} = \int \exp \mathrm{i}(k_x x + k_y y)\, q(x, y)\, \mathrm{d}x\, \mathrm{d}y$, where $\boldsymbol{k} = (k_x, k_y)$. Another alternative is to replace the continuum vorticity by a lattice model (e.g. Burgers 1929*a*; Robert 1991; Robert & Sommeria 1991, 1992; Miller 1990; Miller *et al.* 1992; Majda & Holen 1997; Turkington 1999), i.e. an expansion in terms of tent functions or finite elements of scale size δ. In the present context the vorticity is replaced by its values on the lattice, $q_i = \int K_i(x, y; x_i, y_i) q(x, y)\, \mathrm{d}x\, \mathrm{d}y$, where the kernel K_i is typically chosen to represent a square lattice with a finite number N of sites located at (x_i, y_i). In general $N = N_x N_y$, where N_x and N_y are the number of lattice points in the x- and y-directions, respectively. We will refer to this discretization as a division into m-cells.

Given a finite-dimensional system one can make various assumptions, e.g. the probabilistic assumptions of 'molecular chaos', but this requires a notion of phase-space volume conservation.

4.2. *Phase space volume and Liouville's theorem*

In classical statistical mechanics one calculates averages over the manifold Γ, and the natural volume element is given by $\prod_{\alpha=1}^{N} \mathrm{d}Q_\alpha \mathrm{d}P_\alpha$. However, for $\mathscr{G}$ the situation is not as straightforward, and so we explore candidates for the analogous volume element.

4.2.1. *Volume element*

The calculation of averages in a statistical theory requires a phase-space measure, $\mathscr{D}q$, which is a sort of volume element for $\mathscr{G}$. The volume element can be interpreted as a probability measure defined on functions that take values between q and $q + \mathrm{d}q$. Averages calculated using the probability measure are functional integrals akin to those used in Feynman's path-integral formulation of quantum mechanics and in field theory (e.g. Schulman 1981; Sundermeyer 1982). The various discretizations introduced above have been employed to give meaning to functional integrals, but the Fourier and lattice models are most common.

For the Fourier discretization, Kraichnan & Montgomery used the volume element $\mathscr{D}q = \prod_{\boldsymbol{k}} \mathrm{d}q_{\boldsymbol{k}}$, where the product is truncated at some maximum wavenumber. Alternatively, the volume element for lattice models is written as $\mathscr{D}q = \prod_i^N \mathrm{d}q_i$, where $\mathrm{d}q_i$ is a volume element associated with the potential vorticity varying from q to $q + \mathrm{d}q$ in a lattice partition (x_i, y_i), and $N = N_x N_y$ is, as above, the number

of lattice sites, which have a scale δ. Here, a total volume element $\mathscr{D}q$ is a product of volume elements of each lattice site $\mathrm{d}q_i$. In the case of a finite small lattice, $\mathrm{d}q_i$ becomes a one-dimensional volume, i.e. $\mathrm{d}q_i = q(x_i, y_i) + \mathrm{d}q(x_i, y_i) - q(x_i, y_i)$ at the lattice point (x_i, y_i) of the physical two-dimensional space. In order for a notion of measure based on phase-space volume to be useful, the volume must be preserved in the course of time.

4.2.2. *Liouville's theorem*

Preservation of phase-space volume is assured by Liouville's theorem, an important theorem of mechanics. As noted above, Burgers and Lee showed that a version of Liouville's theorem applies to the system governing the Fourier amplitudes for the inviscid fluid. For vorticity dynamics the amplitudes satisfy

$$\dot{q}_{\boldsymbol{k}} = \sum_{\boldsymbol{l},\boldsymbol{m}} \frac{\epsilon_{\boldsymbol{klm}}}{|\boldsymbol{l}|^2}(q_{\boldsymbol{l}} - h_{\boldsymbol{l}})\, q_{\boldsymbol{m}}, \tag{4.1}$$

where $h_{\boldsymbol{l}}$ is the Fourier transformation of the beta-effect and $\epsilon_{\boldsymbol{klm}} = \hat{z}\cdot(\boldsymbol{l}\times\boldsymbol{m})\delta(\boldsymbol{k}+\boldsymbol{l}+\boldsymbol{m})$ is completely antisymmetric, i.e. $\epsilon_{\boldsymbol{klm}} = -\epsilon_{\boldsymbol{lkm}} = -\epsilon_{\boldsymbol{mlk}}$ and $\epsilon_{\boldsymbol{kkm}} = \epsilon_{\boldsymbol{klk}} = 0$. Therefore, antisymmetry directly implies Liouville's theorem, $\sum_{\boldsymbol{k}} \partial\dot{q}_{\boldsymbol{k}}/\partial q_{\boldsymbol{k}} \equiv 0$.

Similarly, we have shown directly that a version of Liouville's theorem applies to the lattice model. We recently discovered that this version was anticipated in Burgers (1929*b*). This result was also inferred in Turkington (1999). We assume periodic boundary conditions. The lattice model discretization can be viewed as an expansion of the vorticity in terms of a tent function basis (e.g. Fletcher 1980). Upon multiplying the equation of motion by a basis function, as is typical with Galerkin projection, and representing all derivatives as differences, (3.3) becomes

$$\dot{q}_i = \sum_{j,k} B_{ijk}\psi_j q_k, \tag{4.2}$$

which is an equation for the potential vorticity at the lattice point i. Assuming a periodic lattice, the quantity B_{ijk} is easily seen to be completely antisymmetric, i.e. $B_{ijk} = -B_{jik} = -B_{kji}$ and $B_{iji} = B_{iik} = 0$, just as was the case for $\epsilon_{\boldsymbol{klm}}$. Therefore, Liouville's theorem follows,

$$\sum_i \frac{\partial\dot{q}_i}{\partial q_i} = \sum_{i,j,k} B_{ijk}(M_{ji}q_k + \delta_{ki}\psi_j) = \sum_{i,j}(B'_{iij}q_j + B_{iji}\psi_j) = 0, \tag{4.3}$$

where each term of the last sum vanishes. Here the matrix $\boldsymbol{M}$ represents the inverse Laplacian and $\boldsymbol{B}'$ is another matrix that has the same antisymmetry property as $\boldsymbol{B}$.

4.3. *Canonical equilibrium distribution*

Having defined phase space and verified Liouville's theorem, we are ready to write a partition function and to define phase-space averages. The natural expression for the partition function associated with the canonical (Gibbs) ensemble is

$$\mathscr{Z}_c = \int_{\mathscr{G}} \mathrm{e}^{-\beta H[q]-C[q]}\,\mathscr{D}q\,, \tag{4.4}$$

where H is the Hamiltonian of § 3 and C denotes the infinite family of Casimir invariants. Averages corresponding to (4.4) are given by

$$\langle F\rangle_c = \int_{\mathscr{G}} F[q]\, P_c[q;\beta,\mathscr{C}]\, \mathscr{D}q, \tag{4.5}$$

where F is a functional of q and the phase-space probability density is given by

$$P_c[q;\beta,\mathscr{C}] = \mathscr{Z}_c^{-1} \mathrm{e}^{-\beta H[q]-C[q]}. \tag{4.6}$$

Expressions (4.4) and (4.5) are functional integrals (Schulman 1981; Sundermeyer 1982), and the intent is to give them meaning by discretizing as in § 4.1 and then taking the limit $N \to \infty$ and $\delta \to 0$. Finding unique well-defined results with this procedure for such integrals, with other than quadratic functionals in the exponent, is usually a difficult task. Consequently, a mean field approach has been taken, which we turn to in § 5.

An alternative to the direct evalution of (4.5) is to appeal to the fact that the dynamics of (3.3) is an area-preserving rearrangement (e.g. Lieb & Loss 2001). This means for an initial condition q_0, that the solution at time t is given formally by $q(x,y,t) = q_0(x_0(x,y,t), y_0(x,y,t))$, where $(x_0(x,y,t), y_0(x,y,t))$ are the initial conditions of the characteristics, which satisfy $\partial(x_0,y_0)/\partial(x,y) = 1$. The Casimir invariants are associated with relabelling symmetry (e.g. Salmon 1982; Padhye & Morrison 1996) and possess the same value when evaluated on functions that are related by rearrangement. Thus, if one restricts the domain of integration $\mathscr{G}$ to be rearrangements of a given function, denoted by $\mathscr{G}_{\mathscr{R}}$, then we should obtain the same answer because $\langle F[q]\rangle_{\mathscr{R}} = F[q]$ for functionals with integrands that depend only on q, such as Casimirs and $\exp(C[q])$. Here $\langle\ \rangle_{\mathscr{R}}$ is defined with $P_{\mathscr{R}}[q;\beta] = \mathscr{Z}_{\mathscr{R}}^{-1} \exp(-\beta H[q])$ and $\mathscr{Z}_{\mathscr{R}} = \int_{\mathscr{G}_{\mathscr{R}}} \exp(-\beta H[q])\, \mathscr{D}q$.

5. Mean field approximation and statistical independence

It is well-known that vorticity equations like (3.3), the Vlasov equation, and other transport equations develop fine structure in the course of time. Because of this Lynden-Bell (1967) proposed a coarse-graining procedure to obtain a most probable state. He divided phase space up into hyper-fine cells that are assumed to be capable of resolving the fine structure. These are the m-cells referred to in § 4.1, which have a scale size δ. Experimentally δ is determined by the resolution, but in ideal theory the fine structure can become arbitrarily fine and so a limiting procedure is required. In addition Lynden-Bell (1967) proposed larger cells, which we have called M-cells, that characterize a macroscopic scale Δ. The M-cells contain many m-cells that can be freely exchanged within an M-cell without changing any macroscopic quantity. Thus one is able to count states and obtain an expression for a coarse-grained or mean field entropy that can be maximized subject to constraints. Later, Miller (1990) and Robert & Sommeria (1991) reconstructed and improved this formulation. Miller defined m-cells and M-cells based on scales with the property that the energy averaged over M-cells approximates the energy averaged over m-cells. However, we argue that the most important condition for separating the M-cell and m-cell scale lengths is *statistical independence*, which ensures near independence of the probability densities of M-cells, which are viewed as subsystems, and is associated with near additivity of the constraints. These are crucial properties.

Experimentally the two scales can be demonstrated as in figure 2. Observe in plot (a) of this figure the fine-scale structure in the potential vorticity, while in plot (b)

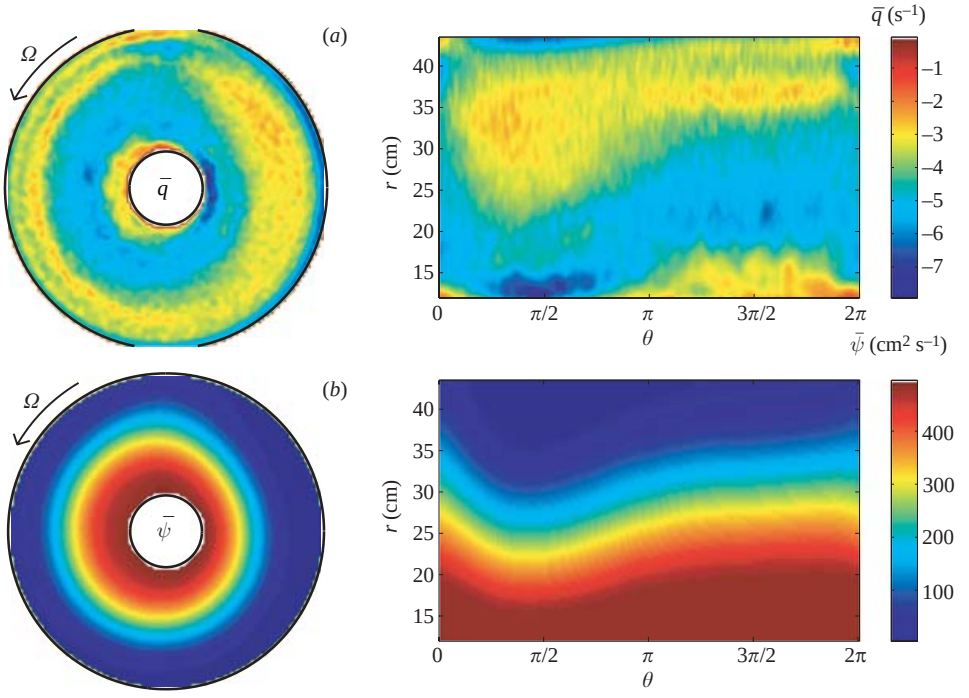

FIGURE 2. The time-averaged potential vorticity (*a*) and the streamfunction (*b*) in the Rossby wave frame. The figures on the left show the fields in the rotating tank; the figures on the right show the same fields unwrapped. The streamfunction field is smoother than the potential vorticity field since the vorticity is given by a second derivative (the Laplacian) of the streamfunction. Hence the characteristic length scale in the azimuthal direction is larger for the streamfunction than for the potential vorticity.

the streamfunction, due to the integration over the Green's function, is considerably smoother. We take the upper scale to be δ and the lower scale to be Δ.

5.1. *Counting states*

According to Lynden-Bell's statistics, the number of ways to distribute m-cells into M-cells is

$$W = \prod_r \frac{N_r!}{\prod_I N_r^{(I)}!} \prod_I \frac{N^{(I)}!}{\left(N^{(I)} - \sum_r N_r^{(I)}\right)!} \tag{5.1}$$

where N_r is the total number of m-cells with the rth value of potential vorticity in the whole space, and $N_r^{(I)}$ is the total number of m-cells with the rth value of potential vorticity in the Ith M-cell. Also, $N^{(I)}$ is the total number of m-cells in the Ith M-cell. The first product in (5.1) represents the number of ways to distribute N_r m-cells into groups of $\{N_r^{(I)}\}$, where I counts all M-cells, and the second product is the number of ways to distribute inside an M-cell. Also, $N^{(I)} - \sum_r N_r^{(I)}$ can be understood as the number of empty m-cells. Lynden-Bell proposed this manner of counting for stellar dynamics (Lynden-Bell 1967, see also Chavanis *et al.* 1996), where m-cells represent stars, which are considered to be distinguishable, and there may be empty m-cells. However, the statistics for the two-dimensional continuum Euler model is a special case of Lynden-Bell's general counting procedure.

In Miller's application to the two-dimensional continuum Euler model, he assumes that all m-cells are occupied by a vortex and these vortices are indistinguishable if they have the same value of vorticity. Because there are no empty m-cells, $N^{(I)} = \sum_r N_r^{(I)}$ and because the m-cells are indistinguishable, a factor of $\prod_r 1/(N_r!)$ is added. This counting produces

$$W = \prod_I \frac{N^{(I)}!}{\prod_r N_r^{(I)}!}. \tag{5.2}$$

The above equation already involves statistical independence among different M-cells.

Boltzmann proposed the entropy as a measure of the number of possible configurations of the system. Therefore, the entropy S is defined to be the logarithm of the total number of configurations, $\ln W$. If $N_r^{(I)}$ is large, Stirling's formula gives

$$S = \ln W \cong -\sum_{r,I} \left(N_r^{(I)}\right) \ln\left(\frac{N_r^{(I)}}{N^{(I)}}\right). \tag{5.3}$$

In the continuum limit of potential vorticity levels, $N_r^{(I)}/N^{(I)}$ is replaced by $P_M(\zeta; x, y)$, and $\sum_{r,I}$ by $\int \mathrm{d}\zeta\, \mathrm{d}x\, \mathrm{d}y$. In short, the index I represents the coordinates for the discretized M-cells and the index r represents the ordered level sets of potential vorticity inside the M-cells. Thus, it is replaced by the continuum vorticity variable ζ, the vorticity on an M-cell. With these observations, the resulting total mean field entropy is seen to be

$$S_M[P_M] = -\int P_M(\zeta; x, y) \ln P_M(\zeta; x, y)\, \mathrm{d}\zeta\, \mathrm{d}x\, \mathrm{d}y = -\int \langle \ln P_M \rangle_M\, \mathrm{d}x\, \mathrm{d}y \tag{5.4}$$

where $P_M(\zeta; x, y)$ is the probability density in the mean field approximation. The density $P_M(\zeta; x, y)$ is centred at the point (x, y) and satisfies the normalization $\int P_M \mathrm{d}\zeta = 1$. The integration over $\mathrm{d}x\, \mathrm{d}y$ can be viewed as a sum over the M-cells that cover the domain of the fluid. The second equality of (5.4) follows from the definition $\langle A \rangle_M = \int A P_M\, \mathrm{d}\zeta$, and thus $S_M[P_M]$ can be naturally termed the (mean field) Boltzmann–Gibbs entropy.

In closing this subsection, we reiterate that the potential vorticity variable q is a field variable, a function of coordinates. However, when we introduced the probability density P_M on M-cells, we used ζ, an independent variable, to represent the values of the potential vorticity on an M-cell.

5.2. *Mean field canonical distribution*

Given the mean field entropy S_M we can proceed to obtain the mean field density $P_M(\zeta; x, y)$ as the most probable state by extremization subject to particular mean field constraints. These constraints and their corresponding Langrange multipliers are given as follows:

(*a*) The *Hamiltonian constraint* is obtained by replacing the vorticity variable q in $H[q]$ with its mean field average, to obtain a mean field energy,

$$\begin{aligned} H_M[P_M] &= \frac{1}{2} \int (\zeta P_M(\zeta; x, y) - h)\ \zeta' P_M(\zeta'; x', y') G(x, y; x', y')\, \mathrm{d}\zeta\, \mathrm{d}x\, \mathrm{d}y\, \mathrm{d}\zeta' \mathrm{d}x' \mathrm{d}y' \\ &= \frac{1}{2} \int \langle \psi \rangle_M (\langle \zeta \rangle_M - h)\, \mathrm{d}x\, \mathrm{d}y \end{aligned} \tag{5.5}$$

where $\langle\zeta\rangle_M = \int \zeta P_M \, \mathrm{d}\zeta$ and $\langle\psi\rangle_M$ is defined by

$$\langle\zeta\rangle_M = -\nabla^2\langle\psi\rangle_M + h. \tag{5.6}$$

The Lagrange multiplier associated with this constraint is taken to be the constant value, $-\beta$, where the minus sign is by convention.

(*b*) The *normalization constraint* is $\int P_M \mathrm{d}\zeta = 1$. This is a normalization on each M-cell; thus, although P_M depends on position, the integration does not. Because this is a constraint for each point (x, y), the Lagrange multiplier in this case depends on position. We call it $\gamma(x, y)$, and the quantity that appears in the variational principle is

$$N_M[P_M] = \int \gamma(x, y) P_M(\zeta; x, y) \, \mathrm{d}\zeta \, \mathrm{d}x \, \mathrm{d}y. \tag{5.7}$$

(*c*) The *mean field Casimir constraint*, roughly speaking, contains the information that on average, the area between any two contours of vorticity remains constant in time. More precisely, the quantity $g(\zeta) = \int P_M \, \mathrm{d}x \, \mathrm{d}y$ is taken to be constant. Because this is true for all ζ, the Lagrange multipler μ is likewise a function of ζ and the constraint can be written as

$$C_M[P_M] = -\beta \int \mu(\zeta) g(\zeta) \, \mathrm{d}\zeta = -\beta \int \mu(\zeta) P_M(\zeta; x, y) \, \mathrm{d}\zeta \, \mathrm{d}x \, \mathrm{d}y, \tag{5.8}$$

where the prefactor of $-\beta$ is again by convention. This constraint is the mean field version of the family of Casimir invariants $C[q]$.

Now we are in position to obtain the most probable state by extremizing the quantity $F_M = S_M - \beta H_M + N_M + C_M$, i.e. upon functional differentiation with respect to P_M, $\delta F_M / \delta P_M = 0$ implies

$$P_M(\zeta; x, y; \beta, \mu) = \mathscr{Z}_M^{-1} \mathrm{e}^{-\beta[\zeta\langle\psi\rangle_M - \mu(\zeta)]}, \tag{5.9}$$

where $\mathscr{Z}_M = \int \mathrm{e}^{-\beta[\zeta\langle\psi\rangle_M - \mu(\zeta)]} \, \mathrm{d}\zeta$ and evidently P_M is normalized. Equation (5.9) is the mean field counterpart to (4.6) and could aptly be termed the canonical (Gibbs) mean field distribution. The above variational principle and extremal distribution (5.9) appeared in essence in an appendix of Lynden-Bell (1967).

Given (5.9) we are in a position to calculate $\langle\zeta\rangle_M$ and then substitute the result into (5.6). This gives the mean field Poisson equation,

$$\nabla^2\langle\psi\rangle_M = \mathscr{Z}_M^{-1} \int \zeta \, \mathrm{e}^{-\beta[\zeta\langle\psi\rangle_M - \mu(\zeta)]} \, \mathrm{d}\zeta + h. \tag{5.10}$$

Versions of this equation have been solved in various references (e.g. Robert & Sommeria 1991; Miller 1990; Majda & Holen 1997), but we will not do this here.

We conclude this subsection by giving a heuristic connection between $\langle\ \rangle_M$, a prescription for averaging functions, and $\langle\ \rangle_c$, a prescription for averaging functionals. Consider the functional $q(x', y')$, by which we mean the evaluation of the function q at the point (x', y'), and evaluate

$$\langle q(x', y')\rangle_c = \int_{\mathscr{G}} q(x', y') \, P_c[q; \beta, \mathscr{C}] \, \mathscr{D}q. \tag{5.11}$$

If we rewrite (5.11) as an integral on M-cells, where $q(x', y')$ is $q_{I'}$, write $\mathscr{D}q = \prod_J \mathrm{d}q_J$, and then assume statistical independence of M-cells, $P_c = \prod_I P_I$, we obtain

$$\langle q(x', y')\rangle_c = \int q_{I'} \prod_I P_I \prod_J \mathrm{d}q_J = \int q_{I'} \, P_{I'} \, \mathrm{d}q_{I'} = \int \zeta P_M \mathrm{d}\zeta = \langle\zeta\rangle_M. \tag{5.12}$$

This derivation emphasizes the need for near statistical independence of M-cell subsystems.

5.3. *Ruggedness and additivity*

Classical statistical mechanical treatments of the canonical ensemble allow subsystems to interact and exchange energy, but their interaction is assumed to be weak and the details of the interaction are usually ignored in calculations. Neglect of the interaction energy results in the energy being equal to the sum of the energies of the individual subsystems, i.e. the energy is an additive quantity. In conventional treatments only additive invariants are used in calculating the most probable distributions, and in some treatments (e.g. Landau & Lifshitz 1980) this requirement is explicitly stated. The reason for this is that additive invariants give rise to statistical independence of subsystems. In our treatment of fluids, subsystems are M-cells and so we consider invariants that are additive over these regions. There is a close connection between ruggedness of invariants and the property of additivity. We show that only the rugged invariants are additive, and thus they characterize the statistical properties of M-cells. In § 5.4 and § 5.5 we will see that experimental results support this reasoning.

Kraichnan & Montgomery (1980) Fourier transformed and truncated to obtain a finite-dimensional system. They argued that the truncated remnants of the total vorticity, enstrophy, and energy are the only invariants to be used in a statistical mechanics treatment because these invariants are rugged, i.e. remain invariants of the truncated system. They also appear to be aware that these invariants possess the property of additivity, but they do not emphasize this point. Although Turkington (1999) has argued that this kind of truncation does not properly handle small-scale behaviour, we find that this theory does a fairly good job at predicting the energy spectrum, but we will report on this elsewhere. We argue in general that such invariants are important because they are the only additive invariants. Below we consider a somewhat more general setting.

Because of Parseval's identity, the quadratic invariants are additive and higher order invariants are not. To see this, suppose we define M-cells to be composed of amplitudes of some subsets of Fourier modes, which we denote by κ_I. Then a sum over modes can be done in groupings, i.e. $\sum_{\boldsymbol{k}} = \sum_I \sum_{\kappa_I}$. (This is the idea behind spectral reduction (Bowman, Shadwick & Morrison 1999), a computational method where groupings of Fourier modes (bins) are described by a single representative.) For the quadratic Casimir invariant, the enstrophy, we have

$$C_2 = \int q^2 \,\mathrm{d}x\,\mathrm{d}y = (2\pi)^2 \sum_{\boldsymbol{k}} |q_{\boldsymbol{k}}|^2, \tag{5.13}$$

and defining an M-cell enstrophy by $C_2^{(I)} = (2\pi)^2 \sum_{\kappa_I} |q_{\boldsymbol{k}}|^2$, we obtain $C_2 = \sum_I C_2^{(I)}$. Similarly, the energy can be written as a sum over M-cell energies, $E = \sum_I E^{(I)}$. The linear Casimir invariant $C_1 = \int q \,\mathrm{d}x\,\mathrm{d}y$ merely reduces to the zeroth Fourier coefficient, and is thus in a trivial sense additive. Higher order invariants, $C_n = \int q^n \,\mathrm{d}x\,\mathrm{d}y$ for $n > 2$, have Fourier representations that are not reducible to expressions in terms of a single sum over M-cells.

The discretized lattice model has properties similar to those described above. The quadratic Casimir invariant and energy reduce to sums over a finite number of m-cell lattice variables, q_i, h_i and ψ_i, which are potential vorticity, height, and streamfunction

represented in terms of the kernel function K_i of § 4 as follows:

$$\left.\begin{aligned} C_2 &= \int q^2 \,\mathrm{d}x\,\mathrm{d}y = \sum_{i,j} \int K_i K_j q_i q_j \,\mathrm{d}x\,\mathrm{d}y = \sum_{i,j} q_i Z_{ij} q_j \,, \\ H &= \frac{1}{2}\int q\psi \,\mathrm{d}x\,\mathrm{d}y = \frac{1}{2}\sum_{i,k} \int K_i K_k (q_i - h_i)\psi_k \,\mathrm{d}x\,\mathrm{d}y \\ &= \frac{1}{2}\sum_{i,k} (q_i - h_i) Z_{ik}\psi_k = \sum_{i,j} (q_i - h_i)\hat{Z}_{ij}(q_j - h_j), \end{aligned}\right\} \tag{5.14}$$

where $Z_{ij} = \int K_i K_j \,\mathrm{d}x\,\mathrm{d}y$ and $\hat{Z}_{ij} = \sum_k Z_{ik} M_{kj}$ are symmetric commuting matrices. These invariants are rugged, i.e they are conserved by the finite dynamical system obtained by projection onto the lattice. In addition, because $\boldsymbol{Z}$ and $\hat{\boldsymbol{Z}}$ commute, one can always find an orthogonal matrix $\mathcal{O}$ that satisfies $\boldsymbol{Z} = \mathcal{O}^T \boldsymbol{D} \mathcal{O}$ and $\hat{\boldsymbol{Z}} = \mathcal{O}^T \hat{\boldsymbol{D}} \mathcal{O}$, where $D_{ij} = d_i \delta_{ij}$ and $\hat{D}_{ij} = \hat{d}_i \delta_{ij}$ are diagonal matrices. Defining $q' = q\mathcal{O}$, $h' = h\mathcal{O}$ and $\psi' = \psi\mathcal{O}$, the enstrophy and energy become

$$\left.\begin{aligned} C_2 &= \sum_{i,j} q_i' D_{ij} q_j' = \sum_i d_i (q_i')^2 = \sum_I \sum_{\kappa_I} d_i (q_i')^2 \\ H &= \sum_i \hat{d}_i (q_i' - h_i')^2 = \sum_I \sum_{\kappa_I} \hat{d}_i (q_i' - h_i')^2 \,, \end{aligned}\right\} \tag{5.15}$$

where I is the index for the Ith M-cell and κ_I denotes the set of m-cells in the Ith M-cell.

This coordinate transformation simultaneously diagonalizes the quadratic Casimir invariant and the energy. However, higher-order Casimir invariants are in general not rugged and are in general not simultaneously diagonalizable. Thus, higher order invariants are not additive, which means M-cells share contributions from these invariants. In this sense, invariants of order higher than quadratic are not useful for describing the statistics of M-cells, which by assumption are independent.

5.4. *Statistically independent subsystems*

Now we turn to the question of how to find subsystems, i.e. how to a find a good definition of the M-cells. First we note that flows inside the rotating tank with the sloped bottom have azimuthal undulations in most physical quantities (streamfunction, potential vorticity, etc.), and these undulations have been identified as Rossby waves (del-Castillo-Negrete & Morrison 1992; Solomon *et al.* 1993). In a co-rotating frame, these waves propagate in the rotation direction at constant velocity. Thus, by shifting to a frame moving at the phase velocity of the Rossby wave, we obtain a pattern that is statistically stationary on large scales. For example, the wavy patterns corresponding to the time-averaged streamfunction and potential vorticity are shown in figure 2. As noted before, the streamfunction is fairly smooth, characteristic of the scale Δ, is monotonically decreasing in the radial direction, and describes a strong zonal flow. However, the time-averaged potential vorticity is scattered with fine structure in space, the δ scale, but still has a wavy mean pattern similar to that of the time-averaged streamfunction. So, this suggests that the first step toward defining M-cells is to consider a frame moving at the phase velocity of the Rossby wave.

Having determined the frame, we seek M-cells that are statistically independent. Because strong correlation in a preferential direction might affect the geometry of

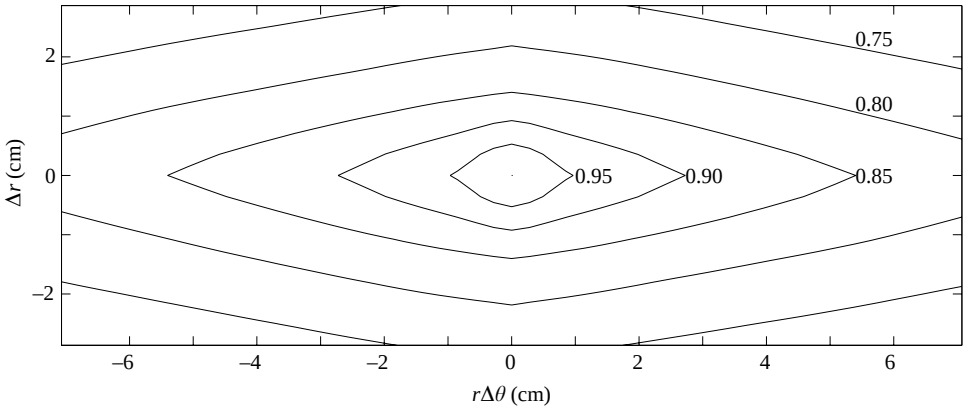

FIGURE 3. Contours of the correlation function $C_{\rm cor}(\Delta r, r\Delta\theta)$ illustrating the anisotropic nature of the potential vorticity field, which has longer range correlation in the azimuathal direction than in the radial direction (cf. figure 2).

M-cells and associated additive invariants, we have measured the correlation function,

$$C_{\rm cor}(\Delta r, r\Delta\theta) = \frac{1}{T}\int_0^T \frac{\int q(r, r\theta\,;t)q(r+\Delta r, r\theta + r\Delta\theta\,;t)r\,\mathrm{d}r\,\mathrm{d}\theta}{\int q(r, r\theta\,;t)^2 r\,\mathrm{d}r\,\mathrm{d}\theta}\,\mathrm{d}t, \tag{5.16}$$

where (θ, r) are the usual polar coordinates. From a large data set of PIV measurements we obtain the time average of the velocity field, whence we calculate the potential vorticity at different positions. Then the integrals of (5.16) are performed with the spatial limits being the bulk of the area occupied by the fluid with a resolution of $\delta \approx 0.8\,\mathrm{cm}$ and the time limit taken to be 80 revolutions with 47 measurements. The result of this procedure is presented in figure 3, which shows contours of $C_{\rm cor}$ plotted on a $(\Delta\theta, \Delta r)$-plane. The highly anisotropic nature of the contours suggests there is significantly less correlation in the radial direction than in the azimuthal direction. Thus to achieve consistent independence the shape of an M-cell should be elongated.

In the course of tracking blobs of fluid we generally observe that to good approximation such blobs follow contours of the time-averaged streamfunction. This, together with the the $C_{\rm cor}$ plot, suggests that a good coordinate for dividing the system into subsystems is the time-averaged streamfunction,

$$\bar{\psi}(r, \theta) = \frac{1}{T}\int_0^T \psi(\theta, r\,;t)\,\mathrm{d}t. \tag{5.17}$$

Contours of $\bar{\psi}$ tend to be smooth and, we argue, are part of a natural coordinate system for describing turbulence with a mean flow that has slow spatial dependence. (We have also considered $\bar{q}$ but found it to be not as good because of its greater variability.) To complete the coordinate system, we introduce a coordinate χ, which is conjugate to $\bar{\psi}$ and therefore satisfies

$$\frac{1}{r}\frac{\partial\bar{\psi}}{\partial\theta}\frac{\partial\chi}{\partial r} - \frac{1}{r}\frac{\partial\bar{\psi}}{\partial r}\frac{\partial\chi}{\partial\theta} = 1. \tag{5.18}$$

Thus the coordinate transformation $(\theta, r) \longleftrightarrow (\chi, \bar{\psi})$ satisfies $r\mathrm{d}r\,\mathrm{d}\theta = \mathrm{d}\chi\,\mathrm{d}\theta$.

We propose that contours of $\bar{\psi}$ define M-cells, which we take to be of small (infinitesimal) width in this coordinate, and we propose that the χ-coordinate at fixed $\bar{\psi}$ represents a continuum of m-cells. We imagine an M-cell to be a region (nearly a curve) at fixed $\bar{\psi}$. Hence with this definition, the probability density $P_{M_{exp}}$, depends only on the potential vorticity variable ζ and on the coordinate $\bar{\psi}$, i.e. $P_{M_{exp}}(\zeta;\bar{\psi})$ is the probability of finding a potential vorticity value ζ in the $\bar{\psi}$ M-cell. Thus the ensemble average of an arbitrary function f is written as

$$\langle f\rangle_{M_{exp}}(\bar{\psi}) = \int f(\zeta,\bar{\psi})P_{M_{exp}}(\zeta;\bar{\psi})\,\mathrm{d}\zeta, \tag{5.19}$$

where $P_{M_{exp}}$ is normalized as $\int P_{M_{exp}}\mathrm{d}\zeta = 1$. In practice we can determine the probability $P_{M_{exp}}$ from data by the relative frequency definition (cf. § 5.5), and then proceed to calculate (5.19). However, this is equivalent to averaging over χ and t, e.g. $\langle\zeta\rangle_{M_{exp}} = \overline{\prec q\succ_\chi}$, where $\prec q\succ_\chi = \int q\,\mathrm{d}\chi/\int\mathrm{d}\chi$. Given $\langle\zeta\rangle_{M_{exp}}$ and using (5.6) to define $\langle\psi\rangle_{M_{exp}}$ we similarly have the equivalence $\langle\psi\rangle_{M_{exp}}(\bar{\psi}) = \overline{\prec\psi(\bar{\psi},\chi;t)\succ_\chi} = \bar{\psi}$, where the second equality follows by definition. The undular streamfunction of figure 2 mainly represents Rossby waves. These wavy patterns are quite robust and often behave as barriers to mixing. In the Rossby wave frame, our data indicate that the instantaneous streamfunction is close to the time-averaged streamfunction, i.e. $\prec\psi(\bar{\psi},\chi;t)\succ_\chi$ deviates from $\bar{\psi}$ by less than 10%. The above comments can be viewed as an experimental verification of ergodicity.

In terms of the above notation the energy and enstrophy densities on M-cells can be written as

$$\left.\begin{aligned}\langle H\rangle_{M_{exp}}(\bar{\psi}) &= \frac{1}{2}\left[\int\zeta\bar{\psi}P_{M_{exp}}(\zeta;\bar{\psi})\,\mathrm{d}\zeta - \prec\bar{\psi}h(\chi,\bar{\psi})\succ_\chi\right]\\ &= \frac{1}{2}\overline{\prec\bar{\psi}[q(\chi,\bar{\psi},t)-h(\chi,\bar{\psi})]\succ_\chi},\\ \langle C_2\rangle_{M_{exp}}(\bar{\psi}) &= \frac{1}{2}\int\zeta^2P_{M_{exp}}(\zeta;\bar{\psi})\,\mathrm{d}\zeta = \frac{1}{2}\overline{\prec q^2(\chi,\bar{\psi},t)\succ_\chi},\end{aligned}\right\} \tag{5.20}$$

and two quantities that measure spatial and temporal fluctuations of these invariants can be compactly written as follows:

$$\Delta_T C_2(\bar{\psi}) = \frac{\left[\overline{(\prec q^2\succ_\chi - \overline{\prec q^2\succ_\chi})^2}\right]^{1/2}}{\overline{\prec q^2\succ_\chi}}, \tag{5.21}$$

$$\Delta_\psi C_2(t) = \frac{\left[\prec(\prec q^2\succ_\chi - \prec q^2\succ_{\chi\bar{\psi}})^2\succ_{\bar{\psi}}\right]^{1/2}}{\prec q^2\succ_{\chi\bar{\psi}}}, \tag{5.22}$$

with similar expressions for $\Delta_T H(\bar{\psi})$ and $\Delta_\psi H(t)$. Figure 4 depicts these quantities. Panel (a) shows temporal fluctuations as a function of the spatial coordinate $\bar{\psi}$. The middle regions of the experiment, where strong zonal flows exist, is describable by statistical mechanics. However, near the walls, corresponding to high and low $\bar{\psi}$ values, statistical mechanics fails because of large fluctuations. Similarly, in panels (b) and (c) the spatial fluctuations are plotted versus time, and it is observed that these fluctuations are quite small. We have measured similar quantities for the cubic and quartic Casimir invariants and the fluctuations are two or three times greater.

An integrated measure of the goodness of our streamfunction-based M-cells is displayed in table 1. Here we have integrated $\prec\Delta_T H\succ_{\bar{\psi}}$ and $\prec\Delta_T C_2\succ_{\bar{\psi}}$ over

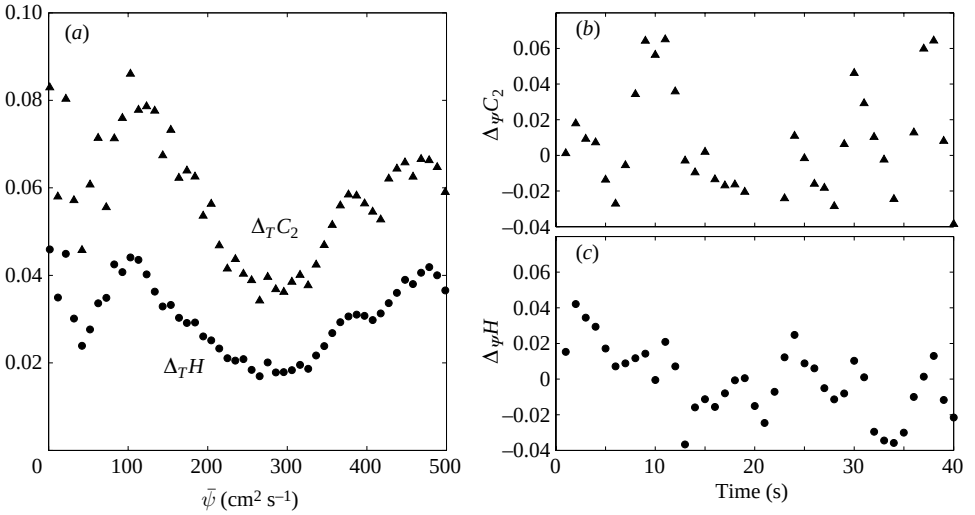

FIGURE 4. (*a*) Enstrophy fluctuations $\Delta_T C_2(\bar{\psi})$ (equation (5.21)) and energy fluctuations $\Delta_T H(\bar{\psi})$ as a function of $\bar{\psi}$. The fluctuations are small, indicating that energy and enstrophy are nearly conserved for our choice of subsystem. (*b*) Total enstrophy variations $\Delta_\psi C_2(t)$ (equation (5.22)) and (*c*) total energy variations $\Delta_\psi H_2(t)$ with time; the variation is small, indicating that the quantities for our choice of subsystem are almost conserved in time.

Fluctuation measure	$\prec \Delta_T H \succ_{\bar{\psi}}$	$\prec \Delta_T C_2 \succ_{\bar{\psi}}$
Square cells	0.2233	0.6425
Streamfunction cells	0.0343	0.0627

TABLE 1. Comparison of fluctuations for square cells with our streamfunction-based cells. Both the energy fluctuation measure $\prec \Delta_T H \succ_{\bar{\psi}}$ and enstrophy fluctuation measure $\prec \Delta_T C_2 \succ_{\bar{\psi}}$ are considerably smaller with the streamfunction-based cells. These small fluctuations allow the division of the system into M-cells, consistent with the statistical independence and additivity assumptions of statistical mechanics.

central values of $\bar{\psi}$ and compared them with counterparts derived using square cells. By this measure, streamfunction-based cells are nearly ten times better than square cells.

Thus, in summary, we have strong evidence supporting the use of streamfunction-based M-cells. The evidence of figure 4 and table 1 imply both statistical independence and the additive nature of the quadratic invariants of these macro-cells.

5.5. *Prediction for PDFs*

Based on the arguments in the previous section, we consider only two invariants out of the infinitely many conserved by the ideal dynamics. Consequently, we obtain the following equilibrium distribution:

$$P_{M_{exp}}(\zeta\,;\bar{\psi}) = \mathscr{Z}^{-1}_{M_{exp}} \exp(-\beta\bar{\psi}\zeta - \gamma\zeta^2), \tag{5.23}$$

where $\mathscr{Z}_{M_{exp}} = \int \exp(-\beta\bar{\psi}\zeta - \gamma\zeta^2)\,\mathrm{d}\zeta$ depends only on $\bar{\psi}$. Note, the function h has cancelled out in the normalization. This probability density function (PDF) has the

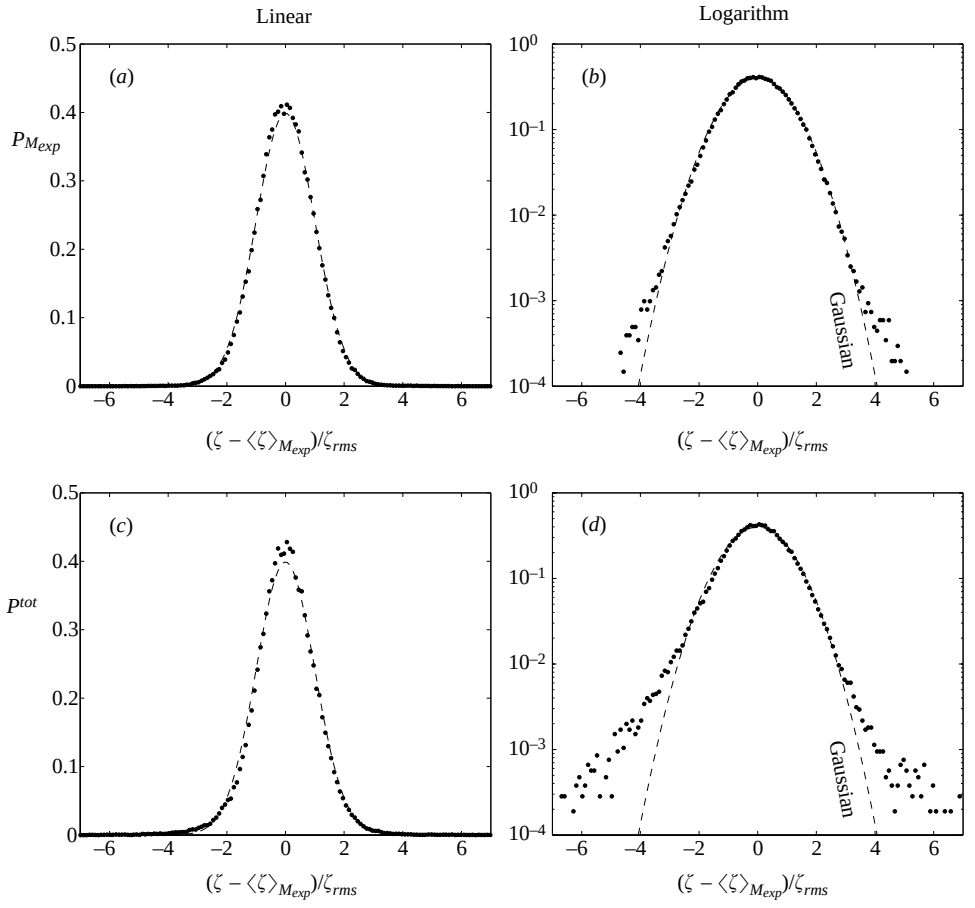

FIGURE 5. The measured probability distribution of potential vorticity (data points) on a typical M-cell is nearly Gaussian (dashed line), in accord with (5.23), as illustrated by these plots on (a) linear and (b) logarithmic scales. In contrast, the potential vorticity of the whole system, shown in (c) and (d) respectively, departs significantly from a Gaussian.

form of a Gaussian that is shifted by $\beta\bar{\psi}/2\gamma$, a position-dependent term that can be interpreted as a sort of 'local wind'.

In figure 5 we compare (5.23) with experimental results. Figures 5(a) and 5(b) show that experimental data on a typical M-cell closely agree with the Gaussian distribution of (5.23). Each distribution is shifted by its mean value of potential vorticity $\langle\zeta\rangle_{M_{exp}}$. Figures 5($c$) and 5($d$) show the total probability $P^{tot}(\zeta)$, which is the sum of the probabilities over all the M-cells, i.e. $P^{tot}(\zeta) = \prec P_{M_{exp}}(\zeta\,;\bar{\psi}) \succ_{\bar{\psi}}$. These plots are decidedly non-Gaussian.

The source of the small deviation in the tails of the distribution plotted in figure 5(b) can be attributed to experimental resolution and sample size. We analysed this by considering the scaling of the skewness and kurtosis with respect to the number of data points N and the experimental subsystem width $\Delta\bar{\psi}$. For a Gaussian distribution the kurtosis is 3 and the skewness is zero. If we fix N (large), our data indicate that the kurtosis approaches 3 as $(\Delta\bar{\psi})^a$, where the exponent a is less than unity and is approximately 0.5 for our last (smallest $\Delta\bar{\psi}$) data points. At fixed $\Delta\bar{\psi}$ (small) we

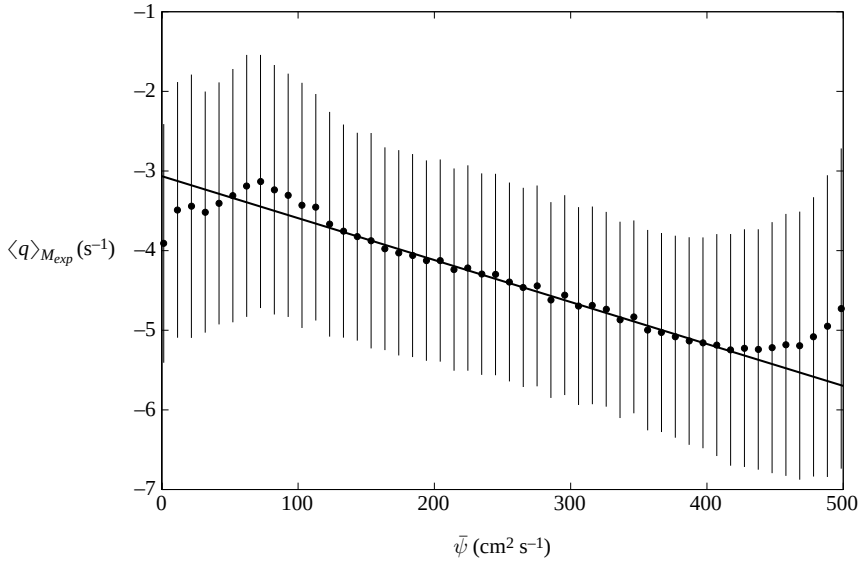

FIGURE 6. The ensemble-averaged potential vorticity $\langle q\rangle_{M_{exp}}$ exhibits a dependence on the time-averaged streamfunction $\bar{\psi}$ that is linear except near the walls (at the ends of the range of $\bar{\psi}$). The dots are mean values of $\langle q\rangle_{M_{exp}}$, and the vertical lines correspond to standard deviations of $\langle q\rangle_{M_{exp}}$ at a fixed $\bar{\psi}$. The data fit well the straight line (a least-squares fit), in accord with the prediction of (5.24), where the slope is the ratio of two Lagrange multipliers.

find that the tails decrease as we increase N. A similar examination of the skewness reveals randomness about the value zero.

The next question is, what is the most probable value of potential vorticity in each M-cell? The probability distribution of (5.23) gives a relation between the averaged vorticity and the streamfunction,

$$\langle\zeta\rangle_{M_{exp}} = \int \zeta\, P_{M_{exp}}(\zeta\,;\bar{\psi})\,\mathrm{d}\zeta = -\epsilon\bar{\psi}, \tag{5.24}$$

which follows by elementary integration. Here $\epsilon = \beta/(2\gamma)$ is the ratio of two Lagrange multipliers. Figure 6 shows a linear relation between the ensemble-averaged potential vorticity $\langle\zeta\rangle_{M_{exp}}$ and the time-averaged streamfunction $\bar{\psi}$, as predicted by (5.24).

Therefore, our theoretical predictions based on a mean field approximation are in good accord with PDFs on M-cells and the averaged values of potential vorticity and streamfunction from experiments. Our theory also indicates that equilibrium can be locally achieved in M-cells, even though the system as a whole is turbulent and non-Gaussian.

6. Conclusions

In this paper we have emphasized the relationship between additive invariants and statistical independence: probability densities that result from entropy maximization principles, such as that of § 5.2, will decompose into a product over subsystems if the entropy is logarithmic (extensive) and the invariants included as constraints are additive over subsystems (M-cells). We have also emphasized that additivity

and, consequently, independence depend on the definition of subsystem. This idea appears, at least implicitly, in conventional statistical mechanics. For example, in the classical calculation of the specific heat of a solid, where one considers a solid to be a collection of lattice sites with spring-like nearest neighbour interactions, the Hamiltonian achieves the form of a sum over simple harmonic oscillators. However, such a diagonal form requires the use of normal coordinates, and only then is the partition function equal to a product over those of the individual oscillators. Thus the notions of subsystem (here a single oscillator), additivity, and statistical independence are intimately related.

In our application of statistical mechanics to inhomogeneous damped and driven turbulence, we have discovered experimentally that a good definition of subsystem is provided by the temporal mean of the streamfunction. With this definition, the quadratic invariants (energy and enstrophy) are additive, and the concomitant probability density of (5.23) agrees quite well with experimental results for both the distribution of vorticity, as depicted in figure 5(*a*, *b*), and the mean state, as depicted in figure 6.

An alternative interpretation of our results can be obtained by the counting argument of § 5.1. Our definition of subsystem amounts to the idea that potential vortices on the same contour of time-averaged streamfunction can exchange their positions with little change in the energy and enstrophy. However, the relocation of two potential vortices that are on different contours of the streamfunction should result in a large change of the invariants. In this sense, the number of possible configurations in phase space can be counted, and the maximization of the entropy so obtained gives our result.

Our discussion of statistical independence and additivity has been heuristic, in the spirit of Boltzmann and Gibbs. We suggest that a more rigorous development could use the techniques described in other works (e.g. Miller *et al.* 1992; Majda & Holen 1997; Turkington 1999) adapted to our $\bar{\psi}$-coordinate that describes our subsystems. For example, one could begin with an appropriate sequence of lattice models and obtain a continuum limit.

Although in this paper we have focused on a geostrophic fluid, our procedure is of general utility and is applicable to physical systems governed by a variety of transport equations. The unifying formalism is the non-canonical Hamiltonian description of § 3, which plays the unifying role played by finite-dimensional canonical Hamiltonian systems in conventional statistical mechanics. Thus we expect our approach to apply to Vlasov–Poisson dynamics, kinetic theories of stellar dynamics, drift-wave plasma models, and other single-field models that possess the non-canonical Poisson bracket of (3.5). Generalization to multi-field models such as reduced magnetohydrodynamics, stratified fluids, and a variety of physics models governed by generalization of the Poisson bracket (Thiffeault & Morrison 2000) of (3.5) provides an avenue for further research.

P.J.M. was supported by the US DOE Grant DE–FG03–96ER–54346. S.J. and H.L.S were supported by ONR Grant N000140410282, and S.J. also acknowledges the support of the Donald D. Harrington Fellows Program of The University of Texas.

REFERENCES

Aubert, J., Jung, S. & Swinney, H. L. 2002 Observations of zonal flow created by potential vorticity mixing in a rotating fluid. *Geophys. Res. Lett.* **29**, 1876.

Baroud, C. N., Plapp, B. B., She, Z. S. & Swinney, H. L. 2002 Anomalous self-similarity in a turbulent rapidly rotating fluid. *Phys. Rev. Lett.* **88**, 114501.

Baroud, C. N., Plapp, B. B., Swinney, H. L. & She, Z. S. 2003 Scaling in three-dimensional and quasi-two-dimensional rotating turbulent flows. *Phys. Fluids* **15**, 2091–2104.

Boucher, C., Ellis, R. S. & Turkington, B. 2000 Derivation of maximum entropy principles in two-dimensional turbulence via large deviations. *J. Statist. Phys.* **98**, 1235–1278.

Bouchet, F. & Sommeria, J. 2002 Emergence of intense jets and Jupiter's Great Red Spot as maximum-entropy structures. *J. Fluid Mech.* **464**, 165–207.

Bowman, J. C., Shadwick, B. A. & Morrison, P. J. 1999 Spectral reduction: a statistical description of turbulence. *Phys. Rev. Lett.* **83**, 5491–5494.

Burgers, J. M. 1929*a* On the application of statistical mechanics to the theory of turbulent fluid motion I. *Koninklijke Nederlandse Akad. Wetenschappen.* **32**, 414.

Burgers, J. M. 1929*b* On the application of statistical mechanics to the theory of turbulent fluid motion II. *Koninklijke Nederlandse Akad. Wetenschappen.* **32**, 632.

Burgers, J. M. 1929*c* On the application of statistical mechanics to the theory of turbulent fluid motion III. *Koninklijke Nederlandse Akad. Wetenschappen.* **32**, 818.

Burgers, J. M. 1933*a* On the application of statistical mechanics to the theory of turbulent fluid motion IV. *Koninklijke Nederlandse Akad. Wetenschappen.* **36**, 276.

Burgers, J. M. 1933*b* On the application of statistical mechanics to the theory of turbulent fluid motion V. *Koninklijke Nederlandse Akad. Wetenschappen.* **36**, 390.

Burgers, J. M. 1933*c* On the application of statistical mechanics to the theory of turbulent fluid motion VI. *Koninklijke Nederlandse Akad. Wetenschappen.* **36**, 487.

Burgers, J. M. 1933*d* On the application of statistical mechanics to the theory of turbulent fluid motion VII. *Koninklijke Nederlandse Akad. Wetenschappen.* **36**, 620.

del-Castillo-Negrete, D. & Morrison, P. J. Hamiltonian chaos and transport in quasigeostrophic flows. In *Research Trends in Physics: Chaotic Dynamics and Transport in Fluids and Plasmas* (ed. I. Prigogine), pp. 181–207. American Institute of Physics.

Chavanis, P. H., Sommeria, J. & Robert, R. 1996 Statistical mechanics of two-dimensional vortices and collisionless stellar systems. *Astro. J.* **471**, 358–399.

Ehrenfest, P. & Ehrenfest, T. 1959 *The Conceptual Foundations of the Statistical Approach in Mechanics.* Cornell University Press. (Translated and revised reissue of *Encyklopädie der mathematischen Wissenschaften, Leipzig*, 1911, **VI** art. 32.)

Ellis, R. S., Haven, K. & Turkington, B. 2002 Nonequivalent statistical equilibrium ensembles and refined stability theorems for most probable flows. *Nonlinearity* **15**, 239–255.

Eyink, G. L. & Spohn, H. 1993 Negative temperature states and large-scale, long-lived vortices in two-dimensional turbulence. *J. Statist. Phys.* **70**, 833–886.

Eyink, G. L. & Sreenivasan, K. R. 2006 Onsager and the theory of hydrodynamic turbulence. *Rev. Mod. Phys.* **78**, 87–135.

Fletcher, C. A. J. 1980 *Computational Techniques for Fluid Dynamics.* Springer.

Joyce, G. & Montgomery, D. 1973 Negative temperature states for the two-dimensional guiding center plasma. *J. Plasma Phys.* **10**, 107–121.

Jung, S., Storey, B. D., Aubert, J. & Swinney, H. L. 2004 Nonextensive statistical mechanics for rotating quasi-two-dimensional turbulence. *Physica* D **193**, 252–264.

Kirchhoff, G. 1883 *Vorlesungen über Mathematische Physik,* vol. 1. Teubner, Leipzig.

Kraichnan, R. H. 1967 Inertial ranges in two-dimensional turbulence. *Phys. Fluids* **10**, 1417–1423.

Kraichnan, R. H. 1975 Statistical dynamics of two-dimensional flow. *J. Fluid Mech.* **67**, 155–175.

Kraichnan, R. H. & Montgomery, D. 1980 Two-dimensional turbulence. *Rep. Prog. Phys.* **43**, 548–618.

Landau, L. D. & Lifshitz, E. M. 1980 *Statistical Mechanics.* Butterworth-Heinemann.

Lee, T. D. 1952 On some statistical properties of hydrodynamical and magneto hydrodynamical fields. *Q. Appl. Maths* **10**, 69–74.

Leith, C. E. 1984 Minimum enstrophy vortices. *Phys. Fluids* **27**, 1388–1395.

Lieb, E. H. & Loss, M. 2001 *Analysis*, 2nd Edn. Chap. 3. American Math. Soc.

Lynden-Bell, D. 1967 Statistical mechanics of violent relaxation in stellar systems. *Mon. Not. R. Astron. Soc.* **136**, 101–121.

McWilliams, J. C. 1984 The emergence of isolated coherent vortices in turbulent flow. *J. Fluid Mech.* **146**, 21–43.

Majda, A. J. & Holen, M. 1997 Dissipation, topography, and statistical theories for large-scale coherent structure. *Comm. Pured Appl. Maths* **50**, 1183–1234.

Marcus, P. S. 1993 Jupiter's Great Red Spot and other vortices. *Annu. Rev. Astron. Astrophys.* **31**, 523–573.

Matthaeus, W. H., Stirbling, W. T., Martinez, D., Oughton, S. & Montgomery, D. 1991 Decaying two-dimensional Navier-Stokes turbulence at very long times. *Physica* D **51**, 531–538.

Maxworthy, T. 1984 The dynamics of a high-speed Jovian jet. *Planet. Space Sci.* **32**, 1053–1058.

Meyers, S. D., Sommeria, J. & Swinney, H. L. 1993 Laboratory study of the dynamics of jovian-type vortices. *Physica D* **37**, 515–530.

Miller, J. 1990 Statistical mechanics of Euler equations in 2-D. *Phys. Rev. Lett.* **65**, 2137–2140.

Miller, J., Weichman, P. B. & Cross, M. C. 1992 Statistical mechanics, Euler's equation, and Jupiter's red spot. *Phys. Rev.* A **45**, 2328–2359.

Morrison, P. J. 1980 The Maxwell-Vlasov equations as a continuous Hamiltonian system. *Phys. Lett.* A **80**, 383–386.

Morrison, P. J. 1981*a* Hamiltonian field description of two-dimensional vortex fluids and guiding center plasmas. *Princeton University Plasma Physics Laboratory Rep. PPPL-1783*;

Morrison, P. J. 1981*b* Hamiltonian field description of the one-dimensional Poisson-Vlasov equation. *Princeton University Plasma Physics Laboratory Rep. PPPL-1788.* Available as American Institute of Physics Document Nos. PAPS-PFBPE-04-771-24 and PAPS-PFBPE-04-771-14, AIP Auxiliary Publication Service, 335 East 45th Street, New York, NY 10017.

Morrison, P. J. 1982 Poisson brackets for fluids and plasmas. In *Mathematical Methods in Hydrodynamics and Integrability in Related Dynamical Systems.* AIP Conference Proceedings 88 (ed. M. Tabor & Y. Treve) P. 13, AIP, New York.

Morrison, P. J. 1998 Hamiltonian description of the ideal fluid. *Rev. Mod. Phys.* **70**, 467–521.

Nieuwstadt, F. T. M. & Steketee, J. A. 1995 *Selected Papers of J.M. Burgers.* Kluwer.

Olver, P. J. 1982 A nonlinear hamiltonian structure for the Euler equations. *J. Math. Anal. Appl.* **89**, 233.

Onsager, L. 1949 Statistical hydrodynamics. *Nuovo Cimento Suppl.* **6**, 279–287.

Padhye, N. & Morrison, P. J. 1996 Fluid element relabeling symmetry *Phys. Lett.* **219**, 287–292.

Robert, R. 1991 A maximum-entropy principle for two-dimensional perfect fluid dynamics. *J. Stat. Phys.* **65**, 531–553.

Robert, R. & Sommeria, J. 1991 Statistical equilibrium states for two-dimensional flows. *J. Fluid Mech.* **229**, 291–310.

Robert, R. & Sommeria, J. 1992 Relaxation towards a statistical equilibrium state in two-dimensional perfect fluid dynamics. *Phys. Rev. Lett.* **69**, 2776–2779.

Rossby, C. G. 1939 Relation between variations in the intensity of the zonal circulation of the atmosphere and the displacements of the semipermanent centers of action. *J. Mar. Res.* **2**, 38–55.

Salmon, R. 1982 Hamilton's principle and Ertel's theorem. In *Mathematical Methods in Hydrodynamics and Integrability in Related Dynamical Systems*, AIP Conference Proceedings No. **88** (ed. M. Tabor & Y. Treve), p. 127. AIP, New York

Salmon, R., Holloway, G. & Henderschott, M. C. 1976 The equilibrium statistical mechanics of simple quasi-geostrophic models. *J. Fluid Mech.* **75**, 691–703.

Schulman, L. S. 1981 *Techniques and Applications of Path Integration.* John Wiley & Sons.

Solomon, T., Holloway, W. J. & Swinney, H. L. 1993 Shear flow instabilities and Rossby waves in barotropic flow in a rotating annulus. *Phys. Fluids* A **5**, 1971–1982.

Sommeria, J., Meyers, S. D. & Swinney, H. L. 1988 Laboratory simulation of Jupiter's Great Red Spot. *Nature* **331**, 689–693.

Sommeria, J., Meyers, S. D. & Swinney, H. L. 1991 Experiments on vortices and Rossby waves in eastward and westward jets. In *Nonlinear Topics in Ocean Physics* (ed. A. Osborne), pp. 227–269. North-Holland.

Sundermeyer, K. 1982 *Constrained Dynamics.* Springer.

Thiffeault, J.-L. & Morrison, P. J. 2000 Classification of Casimir invariants of Lie-Poisson brackets. *Physica* D **136**, 205–244.

Turkington, B. 1999 Statistical equilibrium measures and coherent states in two-dimensional turbulence. *Commun. Pure Appl. Maths* **52**, 781–809.

Van Kampen, N. G. & Felderhof, B. U. 1967 *Theoretical Methods in Plasma Physics.* North-Holland.

Yin, Z., Clercx, H. J. H. & Montgomery, D. C. 2004 An easily implemented task-based parallel scheme for the Fourier pseudospectral solver applied to 2D Navier-Stokes turbulence. *Computers Fluids* **33**, 509–520.